Many-body tight-binding model for aluminum nanoparticles

Grażyna Staszewska*

Institute of Physics, Nicolaus Copernicus University, ul. Grudziadzka 5, 87-100 Toruń, Poland

Przemysław Staszewski*

Department of Theoretical Foundations of Biomedical Sciences and Medical Informatics, Collegium Medicum,
Nicolaus Copernicus University, ul. Jagiellońska 13, 85-067 Bydgoszcz, Poland

Nathan E. Schultz and Donald G. Truhlar

Department of Chemistry and Supercomputing Institute, University of Minnesota, Minneapolis, Minnesota 44455-0431, USA

A new, parametrized many-body tight-binding model is proposed for calculating the potential energy surface for aluminum nanoparticles. The parameters have been fitted to reproduce the energies for a variety of aluminum clusters (Al_2, Al_3, Al_4, Al_7, Al_{13}) calculated recently by the PBE0/MG3 method as well as the experimental face-centered-cubic cohesive energy, lattice constant, and a small set of Al cluster ionization potentials. Several types of parametrization are presented and compared. The mean unsigned error per atom for the best model is less than 0.03 eV.

PACS number(s): 73.22.−f, 81.05.Bx, 31.15.Ct, 36.40.−c

I. INTRODUCTION

The goal of the present paper is to parametrize the tight-binding method[1–10] for the energetic properties of Al particles of nanometer size. Nanoparticles are, in general, too big to be treated by full quantum mechanical methods, but they are too small to neglect the dependence of their quantum properties on size. Because nanostructured materials can have different properties from the bulk, and indeed, due to the large fraction of surface atoms, may be closer in many respects to clusters, the existing tight-binding parametrizations, and other semiempirical methods, since they are usually based on bulk properties, may be less accurate for nanoparticles than for the bulk. Due to experimental difficulties in obtaining well-characterized nanoaluminum, one must rely on theory in developing potential energy functions, and we will base our parametrization mainly on computational results for Al clusters of subnanometer size. However, to make the extrapolation to the nanoparticle regime more accurate, we also include data for the cohesive energy of bulk aluminum in its most stable crystal habit (face-centered cubic) to tie down the asymptote of the extrapolation. In the tight-binding method the matrix elements of an effective single-particle Hamiltonian are modeled as functions of internuclear distances, with adjustable parameters. The quality of a tight-binding parametrization depends strongly on the nature and the quality of the data to which the parameters are fitted as well as on the functional forms used for the matrix elements. The data can be taken from experiment or from accurate calculations. We believe that a set of 190 energies obtained recently for a variety of aluminum clusters[11] (Al_2, Al_3, Al_4, Al_7, Al_{13}), augmented by the experimental cohesive energy and lattice constant, is sufficiently diverse to serve as a training data set for a useful tight-binding parametrization. We believe that this set of data can also be used to verify if the functional forms used are adequate for the system modeled.

Traditionally, each tight-binding matrix element is a function only of the distance between the centers of the two orbitals involved in that matrix element, but our goal here is to study tight-binding models that go beyond the two-center approximation.[12–15] Such models will be called many-body tight-binding models. This approach can be especially useful for the description of nanoparticles where the number of surface atoms is relatively large, and many (or even most) atoms have coordination numbers differing from their bulk value.[16]

II. THEORY

We consider a particle consisting of N nuclei and n electrons. Relativistic effects are neglected, and we assume that the Born-Oppenheimer approximation is valid; then the potential energy for nuclear motion is given by the eigenvalue E of the electronic Hamiltonian $\mathcal{H}$ including the nuclear repulsion,

$$\mathcal{H}\Psi(\mathbf{r}_{\text{electrons}};\mathbf{R}) = E(\mathbf{R})\Psi(\mathbf{r}_{\text{electrons}};\mathbf{R}), \quad (1)$$

where $\mathbf{R}$ and $\mathbf{r}_{\text{electrons}}$ are the coordinates of all the nuclei and electrons, respectively. In (1) the wave functions Ψ and eigenvalues E depend parametrically on the positions of nuclei. By invoking an independent-particle model, the wave function is approximated by a suitably antisymmetrized linear combination of the product of n one-electron functions ψ_i, and Eq. (1) can be converted into a system of nonlinear differential or integrodifferential equations for single-particle (i.e., one-electron) functions:

$$H\psi_i(\mathbf{r};\mathbf{R}) = \varepsilon_i(\mathbf{R})\psi_i(\mathbf{r};\mathbf{R}), \quad i = 1, \dots, n, \quad (2)$$

where ψ_i is an orbital, ε_i is an orbital eigenvalue, and $\mathbf{r}$ is the coordinate of a single electron. The particular form of the effective Hamiltonian operator, H, depends on the choice of independent-particle model, e.g., Hartree-Fock or Kohn-Sham density functional theory (DFT). The latter is more

accurate in principle because it includes electron correlation effects. Tight-binding may be considered as an approximation to DFT with the effective Hamiltonian represented by a matrix Hamiltonian in a minimum basis of valence atomic orbitals. One of the goals of the present paper is to propose a new functional form for this matrix Hamiltonian.

If the one-electron functions, ψ_i, are expanded in a basis of n_α normalized atomic orbitals on each atom α,

$$\psi_i = \sum_{\alpha=1}^{m} c_{i\alpha}\varphi_\alpha(\mathbf{r},\mathbf{R}), \quad m = Nn_\alpha, \tag{3}$$

the set of equations (2) is equivalent to the system of linear homogeneous equations

$$\sum_{p=1}^{m} [H_{pq}(\mathbf{R}) - \varepsilon_i S_{pq}(\mathbf{R})]c_{ip}(\mathbf{R}) = 0, \quad q = 1, \ldots, m, \tag{4}$$

where H_{pq} are matrix elements of H

$$H_{pq} = \int \varphi_p(\mathbf{r},\mathbf{R})H\varphi_q(\mathbf{r},\mathbf{R})d\tau, \tag{5}$$

and

$$S_{pq} = \int \varphi_p(\mathbf{r},\mathbf{R})\varphi_q(\mathbf{r},\mathbf{R})d\tau \tag{6}$$

are elements of the overlap matrix. The matrix elements of **H** and **S** will be denoted by $H_{ij}^{\alpha\beta}$ and $S_{ij}^{\alpha\beta}$, respectively, where i and j refer to atomic orbitals, with i on α (since it is written under α) and j on β (when it is written under β).

The overlap matrix elements involve at most two centers and are often approximated by the unit matrix, which is called neglect of overlap. A guide to the form of the Hamiltonian matrix elements can be obtained by following Slater and Koster,[1] who gave arguments why the three-center integrals in (5) need not be taken into account. Then the matrix elements $H_{ij}^{\alpha\beta}$ for $\alpha \neq \beta$ are functions of $R_{\alpha\beta}$. Considering the vector $\mathbf{R}_{\alpha\beta}$ from α to β as a quantization axis, the interatomic matrix elements can be written in the Slater-Koster approximation in the form

$$H_{ij}^{\alpha\beta} = \sum_{\lambda=0}^{\min(l_i,l_j)} C_{l_i l_j \lambda}^{\alpha\beta}(l_{\alpha\beta},m_{\alpha\beta},n_{\alpha\beta})V_{l_i l_j \lambda}^{\alpha\beta}(R_{\alpha\beta}), \tag{7}$$

where l_i, l_j are angular momentum quantum numbers of orbitals i and j, λ is the component of angular momentum along the internuclear axis, $C_{l_i l_j \lambda}^{\alpha\beta}(l_{\alpha\beta},m_{\alpha\beta},n_{\alpha\beta})$ are the Slater and Koster coefficients resulting from the angular parts of orbitals, and $l_{\alpha\beta}, m_{\alpha\beta}, n_{\alpha\beta}$ are the direction cosines of $\mathbf{R}_{\alpha\beta}$. The diagonal matrix elements $H_{ij}^{\alpha\alpha}$ are constants in the Slater-Koster formalism. For the minimum basis set of aluminum one must model the following four potential functions $V_{l_i l_j \lambda}$: $V_{000}, V_{010}, V_{110}, V_{111}$ (denoted by some authors $V_{ss\sigma}, V_{sp\sigma}, V_{pp\sigma}, V_{pp\pi}$).

Nevertheless, as anticipated in key references[12–15] mentioned in the introduction, going beyond the two-center approximation can be especially useful for achieving high ac-

curacy, and it will be the major focus of the present paper. Therefore it is important to discuss the physical origin of the many-body corrections to TB theory.

In a general way the need for many-body corrections can be traced to the key assumptions of TB theory, namely, (i) the neglect of two-electron interactions, (ii) the neglect of three-center terms (the interaction of an overlap distribution centered on atoms α and β with the nucleus or core of atom γ) in the one-electron Hamiltonian, (iii) the formulation of the one-electron Hamiltonian without self-consistent-filed (SCF) iterations, and (iv) the neglect of overlap in Eq. (4). In more complete theories, the two-electron Coulomb and exchange integrals include both three-center and four-center contributions, so approximations (i) and (ii) are clear sources of the need for many-body terms.[8] The many-body terms in the TB Hamiltonian may always be reformulated as environmentally dependent two-body terms, and environmental dependence of the two-body interactions is accounted for most naturally by an SCF Hamiltonian that depends on the charge distribution. Thus approximation (iii) is also a clear source of the need for many-body terms. Nevertheless, Nguyen-Manh *et al.*[14] have shown that a good approximation to the environmental dependence of the two-body terms may be derived by a detailed examination of only approximation (iv). Their argument starts by reformulating $(\mathbf{H}-\mathbf{SE})\mathbf{c}$ in Eq. (4) by $(\mathbf{S}^{-1}\mathbf{H}-\mathbf{E})\mathbf{c}$. Thus the effect of overlap is to produce an effective Hamiltonian. [In practice one should use a Hermitian version such as (Ref. 14) $(\mathbf{S}^{-1}\mathbf{H}+\mathbf{HS}^{-1})/2$ or (Ref. 17) $\mathbf{S}^{-1/2}\mathbf{HS}^{-1/2}$.] This is a powerful approach that provides a theoretical prescription for a major part of the many-body effect and justifies the physical argument invoking screening that was introduced in Refs. 12 and 13 for the environmental dependence of the two-body interactions.

In the present work we recognize two additional physical effects that, along with screening, contribute an environmental dependence to the two-body interactions. First is the effect of bond angle change. When bond angles change, the hybridization of the bonding orbitals changes as well. In an SCF treatment, polarization of (say) the p orbital component of an sp^2 hybrid orbital is different than polarization of the p component of an sp^3 hybrid. In addition, the energetic effect of electron correlation depends on hybridization. In a TB calculation these many-body polarization and correlation effects must be reflected in the environmental dependence of the two-body interactions. The final physical effect that we consider is coordination number. As the number of bonds to a given atom increases, its flexibility to use hybrid orbitals effectively for directional bonding decreases, and crowding of ligands changes the electron density and hence the exchange-correlation energy. This many-body effect also contributes an environmental dependence to the two-body interactions. In principle all three effects take place simultaneously, and the effects may be additive or multiplicative or they may interact in a very nonlinear fashion. In keeping with the spirit of TB methods, the physical arguments are used only to motivate the functional forms, but the parameters are found by fitting to experiment. At that stage, a functional form motivated by a given physical effect may be general enough to also represent other physical effects. Furthermore, some physically motivated functional forms are

more effective than others at capturing the true physics, and it is better to keep only the most successful forms in order to keep the parametrization compact and physical. In light of the findings of Ref. 14, one could also introduce some many-body effects by not making approximation (iv), i.e., by using a nonorthogonal formulation. In the present work, though, we employ the orthogonal approach because of its greater computational efficiency for large systems. In fact the considerations of Ref. 14 provide a justification of the many-body orthogonal approach.

Based on these considerations, we will neglect the overlap matrix in (4), replacing it by a unit matrix (although we will use S_{pq} in the process of modeling H_{pq}). Furthermore, matrix elements of the effective Hamiltonian will be modeled as functions of one or more of the internuclear distances $R_{\alpha\beta}$ with some number of adjustable parameters to be fitted to representative data from accurate calculations for small systems and from experimental data for the bulk.

To make the dimension of the matrices in Eq. (4) as small as possible, we use a minimal basis set for the valence electrons only. Thus the basis for each Al atom is one $3s$ orbital and three $3p$ orbitals (of p_x, p_y, p_z symmetry), and $n_\alpha = 4$. The matrices **H** and **S** in (4) consist of 4×4 submatrices $\mathbf{H}^{\alpha\beta}$, $\mathbf{S}^{\alpha\beta}$, where α and β label individual nuclei. Note that some authors[18] have included d orbitals on Al, but that would make the basis 2.25 times larger.

The total energy of the system is given as a sum

$$E = E_{\text{val}}(\mathbf{R}) + E_{\text{rep}}(\mathbf{R}) \qquad (8)$$

of the valence electron energy E_{val} and the repulsive energy E_{rep} (associated with core-core repulsion).

One has

$$E_{\text{val}} = \sum_{k=1}^{m} \left[o_k(\mathbf{R})\varepsilon_k(\mathbf{R}) + u_p \delta_{o_k 2} \right], \qquad (9)$$

where $\delta_{kk'}$ is a Kronecker delta, o_k is the occupation number (0, 1, or 2) of molecular orbital k, ε_k is an eigenvalue of **H**, and u_p, which is greater than zero, is the penalty energy[10,19,20] for doubly occupied orbitals. The molecular orbitals are filled in such a way that the total energy of the system is minimized. The penalty energy is included to approximately describe electron correlation and intraorbital repulsion. The standard TB approximation enforces double occupancy of all molecular orbitals (except for single occupancy of one orbital in systems with an odd number of electrons). The penalty energy is a mechanism to overcome this restriction, and it may be considered to be a non-self-consistent version of the Hubbard on-site term[21] that accounts for the change in Coulombic energy and exchange-correlation energy when an orbital is doubly occupied. The inclusion of the penalty energy means that partial occupancies sometimes lead to lower energies than having all orbitals doubly occupied ones, and we will see that this term allows us to obtain improved multiplicities and improved properties of the electronic wave function upon dissociation of clusters.

The repulsive energy

TABLE I. Data for Al.

Hartree-Fock orbital exponents (Ref. 26)	$\zeta_0 = 2.5935$ Å^{-1}
	$\zeta_1 = 2.5610$ Å^{-1}
Atomic ionization potentials (Ref. 22)	$I_0^A = 10.620$ eV
	$I_1^A = 5.986$ eV
Bulk cohesive energy (Refs.11 and 37)	$E_{\text{Bulk}}^{\text{exp}} = 3.43$ eV
Lattice constant (Ref. 38) at 298 K	$a_{\text{exp}} = 4.0496$ Å

$$E_{\text{rep}} = \sum_{\alpha > \beta}^{N} V_{\text{rep}}^{\alpha\beta}(R_{\alpha\beta}) \qquad (10)$$

is a sum of pairwise repulsive energies between any two atomic cores (consisting of the atomic nucleus and core electrons). The repulsive potential also has empirical parameters. In some parametrizations the two-body repulsion functions depend on the environment of those two atoms.

III. MODELS

The data set of aluminum energies[11] can be used not only for fitting parameters in a given model but also for determining which of two models is more accurate. We have studied several models for the matrix elements, and they can be divided into the following two groups: Slater-Koster-type tight-binding (TB) models based on pairwise matrix elements [a matrix element between an orbital on α and one on β depends only on $R_{\alpha\beta}$ as in Eq. (7)], and many-body tight-binding (MBTB) models in which $V_{l_i l_j \lambda}^{\alpha\beta}$ of Eq. (7) is replaced by a function that depends on the geometry of more than two atoms.

For the repulsive energy (10) we have used the function

$$V_{\text{rep}}^{\alpha\beta} = \frac{A}{R_{\alpha\beta}^u} e^{-BR_{\alpha\beta}}, \qquad (11)$$

where A, B, and u are adjustable parameters.

The off-diagonal elements of **H** are called hopping or transfer integrals. We will approximate transfer integrals in terms of overlap integrals in a minimal basis set of Slater-type orbitals (STOs). The overlap between an STO with angular momentum l_α and exponential parameter $\zeta_{\alpha l_\alpha}$ on atom α and an STO with angular momentum l_β and exponential parameter $\zeta_{\beta l_\beta}$ on atom β will be denoted $S_{l_\alpha l_\beta \lambda}(R_{\alpha\beta} | \zeta_{\alpha l_\alpha}, \zeta_{\beta l_\beta})$, where $\lambda = 0$ for σ symmetry and $\lambda = 1$ for π symmetry.

A. Slater-Koster-type TB models

In Slater-Koster-type TB models, intra-atomic matrix elements are assumed to have the form

$$H_{ij}^{\alpha\alpha} = -I_{l_i}\delta_{ij}, \qquad (12)$$

where I_{l_i} is the atomic or valence-state ionization potential of an electron occupying orbital i. In the present paper we use atomic ionization potentials taken from experiment.[22] These values are given in Table I. Atomic ionization potentials will

be denoted I_l^A.

The simplest approximation for the transfer integrals is the one proposed by Mulliken[23] and employed by Wolfsberg and Helmholtz[24] and Hoffmann[25] but with different parametrizations. In this approximation

$$V_{l_i l_j \lambda}^{\alpha\beta} = -K_{l_i l_j \lambda} \frac{I_{l_i}^A + I_{l_j}^A}{2} S_{l_i l_j \lambda}(R_{\alpha\beta}), \qquad (13)$$

where the $K_{l_i l_j \lambda}$ values in (13) and the exponential parameters $\zeta_{\alpha l_\alpha}$ needed to evaluate the overlap integrals are specified below. Depending on the number of parameters in the formula (13) we will distinguish the following three Slater-Koster-type TB models.

(1) Wolfsberg-Helmholtz (WH) approximation. In this model there is one adjustable parameter K_0 for all four hopping integrals, i.e.,

$$K_{l_i l_j \lambda} = K_0 \qquad (14)$$

and the $\zeta_{\alpha l_\alpha}$ are Hartree-Fock values[26] for atoms. These values are given in Table I.

(2) Extended Wolfsberg-Helmholtz (EWH) approximation. In this model each of the four $K_{l_i l_j \lambda}$ is adjusted independently. The ionization potentials and exponential parameters are as in the WH method.

(3) Optimized Wolfsberg-Helmholtz (OWH) approximation. This model is like the EWH model except that the four $\zeta_{\alpha l_\alpha}$ values are also adjusted for best fit.

Together with parameters in the repulsive potential we have 4, 7, and 11 parameters in the WH, EWH, and OWH models, respectively.

Overlap integrals S_{000}, S_{110}, S_{111} were calculated by an analytic formula, given by Jones,[27] for Slater-type orbitals with equal screening constants. Because of the small difference between the values of Slater orbital exponents ζ_s and ζ_p for Al, this formula was also used in the case of S_{010} integral with the screening constant set to their average, 2.577 25 Å^{-1}. This formula can be written in the form

$$S_{l_i l_j \lambda} = w_{n_i l_i n_j l_j}(\zeta_{l_i l_j} R_{\alpha\beta}) e^{-\zeta_{l_i l_j} R_{\alpha\beta}}, \qquad (15)$$

where n_i is the principal quantum number of orbital i, and, denoting the product $\zeta_{l_i l_j} R_{\alpha\beta}$ by p, one has

$$w_{30300} = 1 + p + \frac{7p^2}{15} + \frac{2p^3}{15} + \frac{2p^4}{75} + \frac{p^5}{225} + \frac{p^6}{1575}, \qquad (16)$$

$$w_{30310} = -\frac{1}{\sqrt{27}}\left(p + p^2 + \frac{12p^3}{25} + \frac{11p^4}{75} + \frac{17p^5}{525} + \frac{p^6}{175}\right), \qquad (17)$$

$$w_{31310} = -1 - p - \frac{9p^2}{25} - \frac{2p^3}{75} + \frac{34p^4}{1575} + \frac{13p^5}{1575} + \frac{p^6}{525}, \qquad (18)$$

$$w_{31311} = 1 + p + \frac{34p^2}{75} + \frac{3p^3}{25} + \frac{31p^4}{1575} + \frac{p^5}{525}. \qquad (19)$$

In Eq. (13) we adopted the Harrison[28] sign convention for $V_{l_i l_j \lambda}^{\alpha\beta}$. To be in agreement with this convention we have changed the sign in (17) and (18) in comparison with Table 1 of Ref. 27.

One can consider the WH approximation to be a version of the extended Hückel (EH) approximation.[25,29] It differs in the parametrization. The most commonly adopted constant value of K in EH is 1.75, and it comes from Hoffmann.[25] The most widely available code[30] for the EH method does not include the repulsion potential. In order to compare the EH parametrization of Ref. 30 to the WH, EWH, and OWH methods, we added a repulsion term and optimized it. (The WH, EWH, and OWH methods all include optimized repulsion terms.) The model employing the EH parameters of Ref. 30 plus our optimized repulsion term is denoted EHR. In Sec. V we compare the results of models (1)–(3) with those from the EHR method, calculated with Ref. 31, which is a Minnesota EHR code.

B. Many-body tight-binding

The characteristic properties of nanoparticles are explained in a general way by the large ratio of the number of surface atoms to the number of interior atoms and the fact that surface atoms have a highly variable environment. In the models based on two-body interactions discussed above (i.e., the models employing the two-center approximation for hopping integrals), the influence of the neighboring atoms on the two-body interaction is neglected. Although some previous work[12–14,32–36] on TB modeling has included many-body effects, this kind of approach is much less studied than the conventional two-center approach proposed by Slater and Koster. In a previous paper[16] we have used analytic potential modeling to identify key many-body effects, and in the present paper we will use the functional forms studied there in TB calculations.

We have studied several TB models with many-body effects. In all of them the intra-atomic elements of **H** are taken to be diagonal and to have the form

TABLE II. Ionization potentials (eV) for Al clusters calculated by the PBE0/MG3 method.

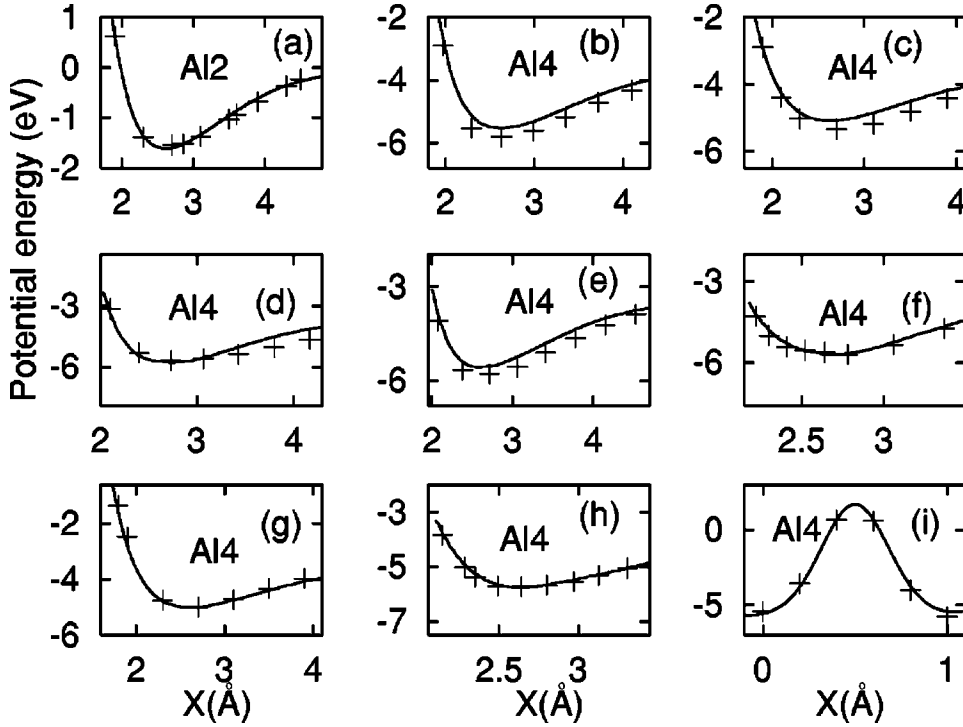| Cluster	Structure No. (Ref. 11)	IP
Al_2	1	7.76
Al_2	3	6.35
Al_3	42	6.55
Al_3	59	6.05
Al_4	3	6.41
Al_4	43	6.38
Al_7	17	6.38
Al_7	34	6.40
Al_{13}	1	6.07

FIG. 1. Potential energies of Al_2 (a) and Al_4 (b)–(i) clusters calculated by MBTB-S method (solid line). Energies denoted by crosses come from the PBE0/MG3 data set. The structures of the clusters are specified by geometry numbers in the supporting material (Ref. 11): (a) 1–10, the dimer; (b) 1–8, short bridge approach of Al to Al_3; (c) 9–16, on top approach of Al to small triangle; (d) 17–24, three-fold approach of Al to small triangle; (e) 25–33, long bridge approach of Al to Al_3; (f) 34–41, dimer-dimer approach; (g) 42–50, on top approach of Al to large triangle; (h) 51–60, threefold approach of Al to large triangle; (i) 61–66, reaction path for conversion of tetrahedron to rhombus.

$$H_{ii}^{\alpha\alpha} = -I_{l_i}^A + \sum_{\substack{\beta \\ (\beta \neq \alpha)}} V_{l_i}(R_{\alpha\beta}), \qquad (20)$$

$$V_l = \Delta_l e^{-\delta_l R_{\alpha\beta}}, \qquad (21)$$

where Δ_l and δ_l are adjustable parameters. Next, the functions $V_{rep}^{\alpha\beta}$, $V_{l_i l_j \lambda}^{\alpha\beta}$, and V_l, given by formulas (11), (13), and (21), respectively, are multiplied by the many-body function F^{MB}, which depends on all internuclear distances except $R_{\alpha\beta}$. We examine three MBTB models.

(1) MBTB based on coordination number (CN). In this

model, $F^{MB} = F^{CN}$, where F^{CN} is a coordination number function defined in Ref. 16. The effective coordination number g_α of atom α is given by the formula

$$g_\alpha = \sum_{\alpha' \neq \alpha} f_g(R_{\alpha\alpha'}), \qquad (22)$$

where

$$f_g(R_{\alpha\alpha'}) = \begin{cases} \exp\left(\gamma_1 + \dfrac{\gamma_1 \gamma_2}{R_{\alpha\alpha'} - \gamma_2}\right) & \text{if } R_{\alpha\alpha'} < \gamma_2, \\ 0 & \text{if } R_{\alpha\alpha'} \geq \gamma_2. \end{cases} \qquad (23)$$

It follows from (23) that only the atoms separated by a distance not exceeding γ_2 are counted, moreover the counts of atoms are weighted by their distances from α. The coordination number function has the form

$$F^{CN} = 1 - d(1 - G_{\alpha\beta}) \qquad (24)$$

with

TABLE III. Multiplicities for quasispherical clusters of sizes N calculated by the PBE0/MEC method and the MBTB-S method for several values of the penalty energy.

N	PBE0/MEC	MBTB-S Penalty energy (eV)		
		0.64	0.07	0.0
13	2	6	2	2
19	6	12	6	2
43	6	18	6	2
55	8	20	2	2
79	2	22	4	2
87	14	30	6	2
135	4	44	2	2
141	10	40	8	2
177	10	54	6	2
MUE		20.44	2.67	4.90

TABLE IV. Comparison of the numbers of cases M_n of neutral dissociation (out of 5460 cases) calculated by MBTB-S method for different penalty energies. (The fitting parameters were optimized for each value of the penalty energy.)

Penalty energy	M_n	%
0.00	0	0
0.07	1015	19
0.64	2323	43

TABLE V. The parameters for pairwise interactions models.

Model No. of parameters	EHR 3	WH 4	EWH 7	OWH 11
A (eV Å^u)	64204	1142	655.5	3069
B (Å^{-1})	10.77	2.921	2.615	3.548
u	0.1880	0.02936	0.0658	0.0955
K_{000} (eV)		0.3928	0.3742	0.3922
K_{010} (eV)		0.3928	0.5181	0.3118
K_{110} (eV)		0.3928	0.3221	0.4292
K_{111} (eV)		0.3928	0.0997	5.934
ζ_{000} (Å^{-1})				1.897
ζ_{010} (Å^{-1})				1.829
ζ_{110} (Å^{-1})				3.876
ζ_{111} (Å^{-1})				6.278

$$G_{\alpha\beta} = \frac{1}{1 + \left(\dfrac{g_a - f_g(R_{\alpha\beta})}{g_0}\right)^\gamma} \frac{1}{1 + \left(\dfrac{g_\beta - f_g(R_{\alpha\beta})}{g_0}\right)^\gamma}. \quad (25)$$

It is convenient to think of g_0 appearing in (25) as a reference coordination number. The function $G_{\alpha\beta}$ takes values between 0 and 1, so the effect of F^{CN} is to weaken the α-β bond. Larger coordination numbers of atoms α and β are associated with weaker α-β Hamiltonian matrix elements, which is a way of explicitly incorporating valence saturation.

There are two positive adjustable parameters, γ and d, for each of the V functions, and three positive adjustable parameters g_0, γ_1, γ_2 which are common for all V functions.

(2) MBTB based on screening (S). In this model, $F^{MB} = F^S$, where F^S is the screening function of Refs. 12 and 13,

$$F^S = 1 - \tanh \xi_{\alpha\beta} \quad (26)$$

with

$$\xi_{\alpha\beta} = \beta_1 \sum_{\delta \neq \alpha,\beta} e^{-\beta_2[(R_{\alpha\delta} + R_{\alpha\beta})/R_{\alpha\delta}]^{\beta_3}}, \quad (27)$$

which includes three-body interactions. There are three positive adjustable parameters, β_1, β_2, β_3, for each of the V functions. The screening function mimics the electronic screening effects such that interaction between two atoms becomes weaker if there is another atom located between them. Like F^{CN}, the screening function F^S varies between 0 and 1, and takes its minimum (the maximum screening effect) when the atom δ is situated on the line connecting atoms α and β.

(3) MBTB with bond-angle (BA) corrections. In this model, $F^{MB} = F^{BA}$ where

$$F^{BA} = 1 - \tanh^{\kappa_4} \chi_{\alpha\beta}, \quad (28)$$

$$\chi_{\alpha\beta} = \kappa_1 \sum_{\gamma, \delta \neq \alpha,\beta} e^{-\kappa_2(R_{\alpha\gamma}^{\kappa_3} + R_{\delta\beta}^{\kappa_3})}. \quad (29)$$

with four positive adjustable environmental parameters, κ_1, κ_2, κ_3, and κ_4, and a different $\chi_{\alpha\beta}$ for each of the V functions, defined in Ref. 16. Equation (28) has one additional parameter, κ_4, in comparison to the original form of the bond-angle function.[16]

The screening and bond-angle functions are closely related; F^{BA}, however, is capable of also modeling four-body

TABLE VI. The parameters for the MBTB-CN model.

	K (eV)	ζ (Å^{-1})		d	γ
V_{000}	0.5781	1.643		0.1290	4.172
V_{010}	0.1880	1.761		0.02061	3.125
V_{110}	0.3371	2.536		0.09656	4.237
V_{111}	0.1252	2.111		0.1768	4.111
	Δ (eV)	δ (Å^{-1})			
V_0	3.017	3.766		0.9002	2.666
V_1	2.246	1.165		0.8997	1.838
	A (eV Å^u)	B (Å^{-1})	u		
V_{rep}	2503	3.503	0.4125	0.1377	2.119
		g_0	γ_1	γ_2	
		12.60	1.692	15.11	

TABLE VII. The parameters for the MBTB-S model.

	K (eV)	ζ (Å^{-1})		β_1	β_2	β_3
V_{000}	0.3577	1.676		0.03723	1.475	0.7413
V_{010}	0.2806	1.785		2.400	4.157	2.252
V_{110}	0.2926	2.570				
V_{111}	0.1990	2.581				
	Δ (eV)		δ (Å^{-1})			
V_0	6.219		3.395			
V_1	2.259		1.137		0.6149	2.813	1.369
	A (eV Å^u)	B (Å^{-1})	u			
V_{rep}	4462	3.896	0.3835			

TABLE VIII. The parameters for the MBTB-BA model.

	K (eV)	ζ (Å^{-1})		κ_1	κ_2 (Å$^{-\kappa_3}$)	κ_3	κ_4
V_{000}	0.2489	1.423		2.827	3.594	1.936	3.647
V_{010}	0.3432	2.150		0.1884	4.324	1.636	2.476
V_{110}	0.2598	2.327					
V_{111}	0.1819	2.486					
	Δ (eV)	δ (Å^{-1})					
V_0	4.540	2.340		0.9586	5.986	1.812	1.592
V_1	3.879	1.369					
	A (eV Å^u)	B (Å^{-1})	u				
V_{rep}	4230	3.889	0.2254				

effects. The maximal weakening of the α-β bond takes place for three-body interaction ($\delta = \gamma$) and atom δ situated on the line connecting atoms α and β. In contrast to F^{CN}, the screening function depends on ratios of the distances, not on the distances between atoms. In particular, the same screening effect is obtained for the atom sitting on the line between α and β independently of the distance $R_{\alpha\beta}$, which is not true for the weakening of the α-β bond due to the bond angle function.

The maximal number of parameters is 32, 36, and 43 in the models MBTB-CN, MBTB-S, MBTB-BA, respectively.

IV. DETERMINATION OF THE PARAMETERS

A. Data

The following data has been used to determine the adjustable parameters in all TB models considered in this paper.

(1) The set of 190 energies calculated by the PBE0/MG3 method for aluminum clusters Al$_2$, Al$_3$, Al$_4$, Al$_7$, and Al$_{13}$.[11] These data were carefully chosen to represent diverse configurations in small as well as in moderate-sized clusters. The coordination number in bulk aluminum is equal to 12, and systems with such coordination numbers are also included in the data in the form of two quasispherical Al$_{13}$ clusters (central atom surrounded by 12 close packed atoms) and one icosahedral cluster. The values of the energies and corresponding Cartesian coordinates, as well as other details of the data set are given in Ref. 11. This set of energies is divided into five cases, i.e., Al$_{N_k}$ with $N_k = 2$, 3, 4, 7, and 13,

for $k = 1, \ldots, 5$, and in case k we have n_k geometries. We will denote the energy for the geometry i of case k by E_i^k. The values of n_k are given in Ref. 11.

(2) Experimental cohesive energy E_{Bulk}^{exp} for a FCC crystal[37] and experimental lattice constant a_{exp} at 298 K,[38] their values are given in Table I.

(3) A set of nine ionization potentials (IP$_i$) calculated by the PBE0/MG3 method for some of the clusters from the set described above. Their values and geometries[11] are given in Table II. The nine geometries for calculating IPs are chosen to represent one high-energy and one low-energy structure for each of the considered clusters.

B. Cohesive energy

The cohesive energy, Q_N, of an N-atom cluster, defined as

$$Q_N = \frac{E}{N} \tag{30}$$

converges rather slowly with N to its bulk limit of E_{Bulk}^{exp} and this dependence can be approximated[39,40] as a linear function of $N^{-1/3}$. Therefore, it is assumed (as in the previous paper[16]) that the bulk cohesive energy E_{Bulk} for an arbitrary value a of the lattice constant can be obtained by computing $Q_N(a)$ for two quasispherical clusters, of sizes N_1 and N_2, with lattice constant a by the extrapolation formula

TABLE IX. Mean unsigned errors in eV/atom and FCC lattice constant a_m in Å.

	ε_2	ε_3	ε_4	ε_7	ε_{13}	ε_{NC}	ε_{Bulk}	ε_{AE}	a_m
EH	0.521	0.589	0.516	0.637	0.718	0.412	3.663	0.745	4.632
EHR	0.417	0.370	0.428	0.452	0.726	0.412	3.692	0.665	4.608
WH	0.040	0.073	0.063	0.050	0.100	0.065	0.126	0.078	4.003
EWH	0.060	0.076	0.071	0.047	0.067	0.065	0.204	0.068	4.035
OWH	0.076	0.080	0.095	0.065	0.031	0.070	0.122	0.058	4.050
MBTB-CN	0.038	0.078	0.050	0.077	0.025	0.049	0.000	0.046	4.050
MBTB-S	0.023	0.065	0.046	0.038	0.013	0.033	0.001	0.029	4.050
MBTB-BA	0.038	0.061	0.042	0.055	0.019	0.031	0.088	0.038	4.050

TABLE X. $|\Delta E_i^k|$ (eV/atom).

Structure No. (Ref. 11)	Reaction coordinate	WH	OWH	MBTB-S	MBTB-BA
		Al$_2$			
1	1.90	0.05	0.13	0.01	0.15
2	2.30	0.12	0.15	0.03	0.13
3	2.70	0.09	0.27	0.06	0.00
4	2.86	0.03	0.31	0.00	0.04
5	3.10	0.04	0.29	0.04	0.06
6	3.50	0.11	0.23	0.07	0.06
7	3.60	0.11	0.21	0.07	0.06
8	3.90	0.10	0.15	0.06	0.04
9	4.30	0.04	0.05	0.01	0.02
10	4.50	0.00	0.01	0.04	0.06
		Al$_3$, oblique approach to large dimer			
29	6.06	0.37	0.16	0.15	0.12
30	5.71	0.36	0.26	0.06	0.00
31	5.36	0.44	0.09	0.13	0.02
32	5.02	0.35	0.03	0.08	0.03
33	4.68	0.32	0.03	0.07	0.00
34	4.35	0.29	0.04	0.09	0.03
35	4.02	0.14	0.03	0.09	0.00
36	3.71	0.02	0.17	0.07	0.05
37	3.56	0.08	0.18	0.13	0.02
38	3.41	0.01	0.32	0.05	0.04
39	3.12	0.01	0.41	0.06	0.01
		Al$_{13}$			
1		1.02	0.65	0.04	0.21
2		0.93	1.01	0.20	0.33
3		0.91	0.25	0.19	0.10
4		0.22	0.28	0.25	0.29
5		0.00	0.10	0.04	0.14
6		1.09	0.41	0.10	0.28
7		0.74	0.06	0.25	0.28
8		1.83	0.38	0.21	0.30
9		1.94	0.19	0.20	0.03
10		0.41	0.02	0.03	0.02
11		2.74	0.15	0.18	0.40

$$E_{\text{Bulk}}(a) = \frac{N_1^{-1/3} Q_{N_2}(a) - N_2^{-1/3} Q_{N_1}(a)}{N_1^{-1/3} - N_2^{-1/3}}. \qquad (31)$$

As in Ref. 16, we used $N_1 = 55$, $N_2 = 321$. For the fitting procedure of the TB potential parameters we made use of two cohesive energies E_{Bulk} for two lattice constants: the experimental lattice constant a_{exp} and the minimum-energy lattice constant a_m. The two energies are denoted by $E_{\text{Bulk}}(a_{\text{exp}})$ and $E_{\text{Bulk}}(a_m)$. The lattice constant a_m is obtained by minimizing $E_{\text{Bulk}}(a)$, for a given set of TB or MBTB parameters, with respect to a.

C. Penalty energy

We optimized the value of the penalty energy of Eq. (9) in the following way. First, for our best TB model (MBTB-S) the fitting parameters of the potentials were optimized for several values of the penalty energy. The values of the multiplicity of the clusters were found to strongly depend on the penalty energy. Therefore, the final choice of the penalty energy was made by minimizing the mean unsigned error (MUE) in the multiplicities over a set of data calculated by a recently developed version of hybrid density functional method (PBE0/MEC, which denotes the Perdew-Burke-Ernzerhof method with zero empirical parameters and the

TABLE XI. ε_{IP} (eV).

EH	1.06
EHR	1.06
WH	0.58
EWH	0.31
OWH	0.36
MBTB-CN	0.30
MBTB-S	0.36
MBTB-BA	0.39

Minnesota effective core).[41,42] The multiplicities obtained by the PBE0/MEC method and by TB methods with different penalty energies, and the corresponding MUEs are given in Table III. The optimum value, used in the present paper, is 0.07 eV. Two sets of fitting parameters optimized for other penalty energies, namely 0.0 eV and 0.64 eV, are given in the supporting information file.[43] These models with other penalty energies may be useful for various purposes (e.g., a penalty energy of zero is easier to handle in dynamics calculations, and a larger penalty energy may be a better starting point for adding heteroatoms), but these alternatives will not be discussed further in this paper.

It is important to emphasize that the present parametrization is designed to yield accurate nanoparticle energies, but not necessarily nanoparticle wave functions or bulk energies or band structures. As is well known,[45] a double-occupancy molecular orbital method like tight-binding does not necessarily dissociate into a qualitatively correct wave function upon bond cleavage. For example, if a system with an even number of Al atoms dissociates asymmetrically into two fragments which each have an odd number of electrons (for example, $Al_4 \rightarrow Al_3 + Al$), the restriction to doubly occupied orbitals means that one fragment will have a cationic wave function and the other an anionic one. It is important to keep in mind that the present method is nevertheless parametrized yield to reasonably accurate dissociation energies even when this happens. This is a special case of the more general phenomenon that one can obtain correct energetic predictions even from a wave function that does not predict correct electronic properties such as multipole moments. This is especially true when we use the modern justification of TB theory as being an approximation to density functional theory since it is not necessary to interpret the Kohn-Sham orbital eigenvalues as having a direct relation to band theory, at least when we use integer occupancies.[44] The inclusion of a penalty function does, however, represent a step toward improving the behavior of the wave function, and it does allow us to obtain reasonable multiplicities. It also affects the behavior of the wave function upon dissociation, and this deserves a few remarks. The penalty energy can make up in part for the incorrect dissociation of tight-binding wave functions, but not completely. Our data set contains 104 molecules with an odd number of Al atoms, which allows us to create 5460 unique pairs of such molecules, which may in turn be considered as 5460 dissociation asymptotes. Table IV shows the percentage of these asymptotes that correspond to neutral fragment wave functions; we see that this percentage increases, although only slowly, as the penalty energy increases. However, the largest value of the penalty energy in the table leads to an unacceptably large error in the multiplicities, so we chose 0.07 eV as a compromise value for the penalty energy. We recall that Wang and Mak[19] used a penalty energy of 3 eV for hydrocarbon species. That might be

TABLE XII. Cohesive energies in Al_N (eV).

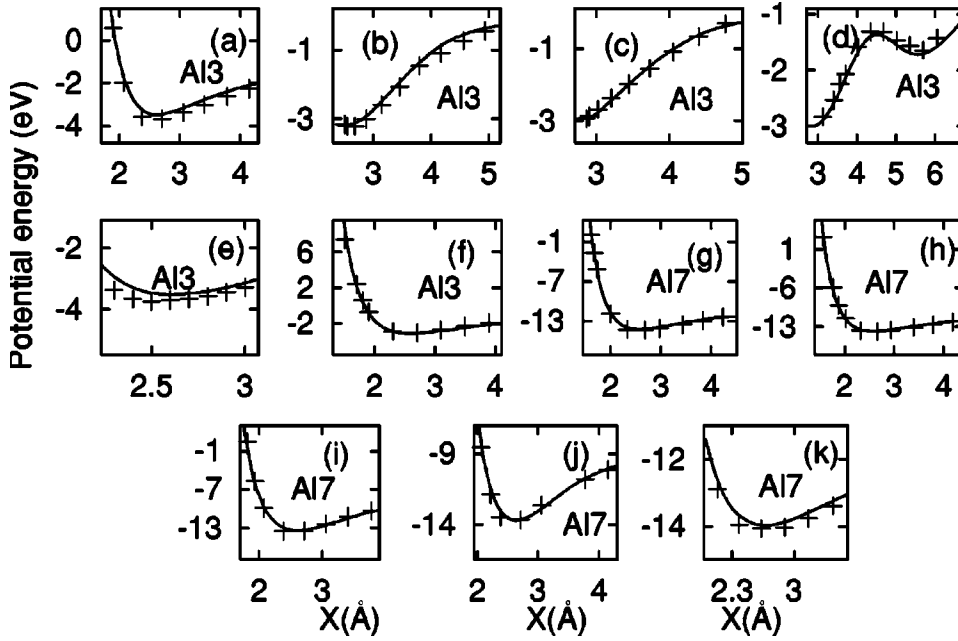| N	WH	EWH	OWH	MBTB-CN	MBTB-S	MBTB-BA
13	2.30	2.31	2.35	2.37	2.38	2.37
19	2.49	2.56	2.52	2.62	2.66	2.59
43	2.72	2.78	2.77	2.80	2.83	2.80
55	2.82	2.92	2.90	2.94	2.94	2.92
79	2.95	3.08	3.01	3.07	3.09	3.04
87	2.89	3.01	2.96	3.04	3.02	2.99
135	3.02	3.12	3.08	3.09	3.10	3.08
141	3.01	3.12	3.07	3.12	3.10	3.08
177	3.06	3.15	3.11	3.12	3.12	3.11
201	3.12	3.20	3.15	3.13	3.16	3.15
225	3.08	3.17	3.13	3.13	3.12	3.14
249	3.10	3.19	3.15	3.12	3.13	3.15
321	3.15	3.24	3.19	3.16	3.16	3.20
369	3.18	3.27	3.21	3.16	3.17	3.22
381	3.17	3.27	3.21	3.16	3.17	3.22
429	3.17	3.27	3.21	3.16	3.17	3.22
531	3.20	3.28	3.23	3.17	3.17	3.24
555	3.21	3.30	3.24	3.17	3.18	3.25
603	3.22	3.31	3.25	3.18	3.19	3.26

FIG. 2. The same as in Fig. 1 but for Al$_3$ (a)–(f), and Al$_7$ (g)–(k). The points are (a) 1–9, sideways approach of Al to small dimer; (b) 10–19, sideways approach of Al to medium dimer; (c) 20–28, sideways approach of Al to large dimer; (d) 29–39, oblique approach of Al to large dimer; (e) 40–47, equilateral triangles; (f) 48–57, linear approach of Al to small dimer; (g) 1–11, approach of Al to small octahedron; (h) 12–22, approach of Al to large octahedron; (i) 23–31, large trimer approaching large tetramer; (j) 32–40, small trimer approaching small tetramer; (k) 41–46, approach of Al to small octahedron along the perpendicular bisector of a bond.

better for dissociation, but is definitely worse for multiplicities.

D. The fitting procedure

A microgenetic algorithm[46] has been applied to the estimation of parameters. We have used the FORTRAN version 1.7a of Carroll's code[47] (updated on 4/2/2001) augmented by a subroutine with our fitness function.

Four groups of terms are included in the fitness function. The first group of terms fits the differences between PBE0/MG3 and TB energies:

$$\Delta\Delta E_{ij}^k = \Delta E_{ij}^k - \Delta E_{ij}^{\mathrm{TB}k}, \tag{32}$$

where

$$\Delta E_{ij}^k = E_i^k - E_j^k, \tag{33}$$

TABLE XIII. Comparison of mean unsigned errors (eV/atom) to previous tight-binding models.

	Nonclose Al data set	Large Al data set
	$\varepsilon_{\mathrm{AE}}$	
EH	0.63	0.75
EHR	0.64	0.67
OWH	0.06	0.06
MBTB-S	0.02	0.03
	$\varepsilon_{\mathrm{Av}}$	
EH	0.52	0.64
EHR	0.53	0.56
TBTE (Ref. 11)	0.36	4.46
OWH	0.06	0.06
MBTB-S	0.03	0.03

$$\Delta E_{ij}^{\mathrm{TB}k} = E_i^{\mathrm{TB}k} - E_j^{\mathrm{TB}k}, \tag{34}$$

and $E_i^{\mathrm{TB}k}$ stand for the energies calculated by the TB method. Notice that throughout this paper the zero of energy for a given k is taken as the energy of n_k separated atoms. The second group of terms fits the energies

$$\Delta E_i^k = E_i^k - E_i^{\mathrm{TB}k}, \tag{35}$$

the third group of terms fits the cohesive energies E_{Bulk} to the bulk experimental value $E_{\mathrm{Bulk}}^{\mathrm{exp}}$ (Table I),

$$\Delta E_{\mathrm{Bulk}}^m = E_{\mathrm{Bulk}}(a_m) - E_{\mathrm{Bulk}}^{\mathrm{exp}},$$

$$\Delta E_{\mathrm{Bulk}}^{\mathrm{exp}} = E_{\mathrm{Bulk}}(a_{\mathrm{exp}}) - E_{\mathrm{Bulk}}^{\mathrm{exp}}. \tag{36}$$

The fourth term fits ionization potentials,

$$\Delta\mathrm{IP}_i = \mathrm{IP}_i - \mathrm{IP}_i^{\mathrm{TB}}. \tag{37}$$

We define a mean unsigned error per atom for Al$_{N_k}$ clusters as

$$\varepsilon_{N_k} = \frac{1}{2N_k}\left[\frac{2}{n_k(n_k-1)}\sum_{i=1}^{n_k-1}\sum_{j=i+1}^{n_k}\left|\Delta\Delta E_{ij}^k\right| + \frac{1}{n_k}\sum_{i=1}^{n_k}\left|\Delta E_i^k\right|\right], \tag{38}$$

where the first (double) summation includes all relative energies of two geometries in the data set, and the second term sums over individual geometries. The mean unsigned error per atom in energies and their differences is then defined as the weighted average

$$\varepsilon_{\mathrm{Clu}} = \frac{1}{N_{\mathrm{Clu}}}\sum_{k=1}^{5} N_k \varepsilon_{N_k}, \tag{39}$$

where

TABLE XIV. Ranges of the two-body functions.

Model	Function f/Distance (Å)	n = 2 4.050	3 4.960	4 5.727	5 6.043	6 7.014
MBTB-S	$V_{000}F^{S}$	1.7×10^{-1}	3.4×10^{-2}	7.9×10^{-3}	2.1×10^{-3}	6.5×10^{-4}
	$V_{010}F^{S}$	7.7×10^{-2}	9.6×10^{-4}	4.5×10^{-6}	1.0×10^{-8}	1.3×10^{-11}
	V_{110}	3.4×10^{-1}	1.0×10^{-1}	3.3×10^{-2}	1.1×10^{-2}	3.8×10^{-3}
	V_{111}	1.7×10^{-1}	3.7×10^{-2}	9.4×10^{-3}	2.7×10^{-3}	8.2×10^{-4}
	V_{rep}	8.6×10^{-3}	2.3×10^{-4}	1.1×10^{-5}	7.5×10^{-7}	6.7×10^{-8}
MBTB-BA	$V_{000}F^{BA}$	6.4×10^{-1}	4.1×10^{-1}	2.2×10^{-1}	1.4×10^{-1}	8.4×10^{-2}
	$V_{010}F^{BA}$	4.3×10^{-1}	1.8×10^{-1}	7.4×10^{-2}	3.2×10^{-2}	1.4×10^{-2}
	V_{110}	4.5×10^{-1}	1.7×10^{-1}	6.6×10^{-2}	2.6×10^{-2}	1.0×10^{-2}
	V_{111}	1.9×10^{-1}	4.5×10^{-2}	1.2×10^{-2}	3.6×10^{-3}	1.2×10^{-3}
	V_{rep}	9.2×10^{-3}	2.5×10^{-4}	1.2×10^{-5}	8.8×10^{-7}	8.0×10^{-8}
MBTB-CN	$V_{000}F^{CN}$	5.5×10^{-1}	3.0×10^{-1}	1.7×10^{-1}	9.8×10^{-2}	5.7×10^{-2}
	$V_{010}F^{CN}$	6.3×10^{-1}	3.5×10^{-1}	1.9×10^{-1}	1.1×10^{-1}	5.9×10^{-2}
	$V_{110}F^{CN}$	3.5×10^{-1}	1.1×10^{-1}	3.6×10^{-2}	1.2×10^{-2}	4.4×10^{-3}
	$V_{111}F^{CN}$	2.8×10^{-1}	8.8×10^{-2}	3.1×10^{-2}	1.2×10^{-2}	4.8×10^{-3}
	$V_{rep}F^{CN}$	1.4×10^{-2}	5.1×10^{-4}	3.3×10^{-5}	2.9×10^{-6}	3.3×10^{-7}
OWH	V_{000}	4.5×10^{-1}	2.1×10^{-1}	1.0×10^{-1}	4.9×10^{-2}	2.5×10^{-2}
	V_{010}	5.9×10^{-1}	3.1×10^{-1}	1.6×10^{-1}	8.6×10^{-2}	4.6×10^{-2}
	V_{110}	7.3×10^{-2}	6.9×10^{-3}	8.1×10^{-4}	1.1×10^{-4}	1.8×10^{-5}
	V_{111}	2.8×10^{-3}	2.3×10^{-5}	3.7×10^{-7}	8.9×10^{-9}	3.0×10^{-10}
	V_{rep}	1.4×10^{-2}	5.6×10^{-4}	3.6×10^{-5}	3.3×10^{-6}	3.7×10^{-7}
EWH	V_{000}	2.4×10^{-1}	6.4×10^{-2}	1.9×10^{-2}	5.9×10^{-3}	2.0×10^{-3}
	V_{010}	2.8×10^{-1}	8.0×10^{-2}	2.4×10^{-2}	7.9×10^{-3}	2.7×10^{-3}
	V_{110}	3.4×10^{-1}	1.1×10^{-1}	3.3×10^{-2}	1.1×10^{-2}	4.0×10^{-3}
	V_{111}	1.8×10^{-1}	3.9×10^{-2}	9.9×10^{-3}	2.8×10^{-3}	8.8×10^{-4}
	V_{rep}	4.4×10^{-2}	4.0×10^{-3}	5.3×10^{-4}	9.1×10^{-5}	1.8×10^{-5}
WH	V_{000}	2.4×10^{-1}	6.4×10^{-2}	1.9×10^{-2}	5.9×10^{-3}	2.0×10^{-3}
	V_{010}	2.8×10^{-1}	8.0×10^{-2}	2.4×10^{-2}	7.9×10^{-3}	2.7×10^{-3}
	V_{110}	3.4×10^{-1}	1.1×10^{-1}	3.3×10^{-2}	1.1×10^{-2}	4.0×10^{-3}
	V_{111}	1.8×10^{-1}	3.9×10^{-2}	9.9×10^{-3}	2.8×10^{-3}	8.8×10^{-4}
	V_{rep}	3.1×10^{-2}	2.2×10^{-3}	2.3×10^{-4}	3.2×10^{-5}	5.3×10^{-6}

$$N_{Clu} = \sum_{k=1}^{5} N_k. \tag{40}$$

The mean unsigned error in the bulk cohesive energies is

$$\varepsilon_{Bulk} = \tfrac{1}{2}\left[|\Delta E_{Bulk}^{m}| + |\Delta E_{Bulk}^{exp}|\right]. \tag{41}$$

The mean unsigned error in atomization energy (AE) per atom for neutral aluminum, ε_{AE}, is defined as the weighted average of ε_{Bulk} and the five values of ε_{N_k},

$$\varepsilon_{AE} = \frac{1}{N_{Neu}}\left(\sum_{k=1}^{5} N_k\varepsilon_{N_k} + \varepsilon_{Bulk}\right), \tag{42}$$

where $N_{Neu}=N_{Clu}+1$. The mean unsigned error for the ionization potentials is

$$\varepsilon_{IP} = \frac{1}{9}\sum_{i=1}^{9} |\Delta IP_i|, \tag{43}$$

and the mean unsigned error for the total data set is

TABLE XV. Comparison of ε_{AE} (eV/atom) for aluminum with analytic potentials to those for tight-binding.

	Analytic (Ref. 16)	TB
Best pairwise	0.32 (ER)	0.06
Best MB	0.05 (ER2+ESCNa)	0.03

$$\varepsilon_{\text{Tot}} = \frac{1}{N_{\text{Tot}}}\left(\sum_{k=1}^{5} N_k \varepsilon_{N_k} + \varepsilon_{\text{Bulk}} + \varepsilon_{\text{IP}}\right), \qquad (44)$$

where $N_{\text{Tot}} = N_{\text{Clu}} + 2$. To minimize the total error we define the fitness function (which is maximized) as

$$f = -\varepsilon_{\text{Tot}}. \qquad (45)$$

To compare our results to previous tight-binding models we also introduce a measure of the average error per atom in the atomization energy in the form of

$$\varepsilon_{\text{Av}} = \frac{1}{5}\sum_{k=1}^{5} \varepsilon_{N_k}. \qquad (46)$$

V. RESULTS AND DISCUSSION

The optimized parameters for six models are given in Tables V–VIII. In two MBTB models the number of parameters shown in Tables VII and VIII is less than the maximal one. This arises as follows. First, in the process of optimization all many-body terms were included and the importance of each term was examined. Some of the correction terms appear not to be important, and they were not taken into account in the further process of optimization. This happened in the S model and BA models where we kept 24 and 27 parameters, respectively, as compared to maxima of 36 and 43, respectively. In both models the many body corrections to V_{110}, V_{111}, and V_{rep} turned out to be insignificant. Also, one correction to the diagonal terms in each model was effectively redundant, but for the S model the correction to V_1 was kept, and for the BA model the correction to V_0 appeared to be significant. The parameters of omitted terms are left blank in Tables VII and VIII.

We also considered models in which combinations of many-body functions were applied, e.g., $F^{\text{MB}} = F^{\text{CN}}F^{S}$ or $F^{\text{MB}} = F^{\text{CN}}F^{\text{BA}}$. Such combinations increase considerably the number of parameters to be optimized but do not significantly improve the fits and therefore are not discussed further.

For all six methods we have computed the mean unsigned error in atomization energy for neutral systems. We have also calculated the ε_{AE} for the extended Hückel method (EH)[29] with and without the repulsion potential term included. The results are given in Table IX. As seen in Table IX, the EH method gives considerably larger error for all cases, and these errors increase for bigger and bigger clusters.

The WH approximation gives much more realistic results than the EHR model. Among the Slater-Koster-type TB models, the OWH method where both linear and nonlinear pa-

TABLE XVI. Timing comparisons (s) for tight-binding methods and analytic potentials from Table XV.

Number of atoms	249	531
TB		
WH	19	193
MBTB-CN	19	251
MBTB-S	64	792
MBTB-BA	22	261
Analytic (Ref. 17)		
ER	0.024	0.10
ER2+ESCNa	0.90	5.9

rameters were optimized, gives a much smaller error ε_{AE} than the others.

As in Refs. 11 and 16 we also consider a nonclose data set of 155 energies which is obtained from our data set of 190 energies by removing all points for which any Al-Al distance is smaller than 2.25 Å; the remaining geometries are the ones with no close (NC) approach of any two atoms.

The values of ε_{Av} for NC data are also given in Table IX. They are denoted in this Table as ε_{NC}. Eliminating the close parts lowers the mean error defined this way by 31% for EH and 12% for EHR, but it has almost no effect on the average errors for the other Slater-Koster-type parametrizations. For the three MBTB methods that have the smallest errors, it lowers the mean unsigned error by 8–24%.

The MBTB methods give better representations of the data than Slater-Koster-type TB methods. The many-body terms are more important for bigger clusters. The comparison between MBTB methods shows that the MBTB-S method is best. In Figs. 1 and 2 we compare potential energies for Al_2, Al_3, Al_4, and Al_7 obtained by MBTB-S method to those obtained by PBE0/MG3 method. To plot each MBTB curve we calculated 100 values of energy. The fit is very good and all the curves are smooth. In the case of Al_{13} the quality of the fit is presented in Table X, where ΔE_i^k is also tabulated for Al_2 and Al_3 (oblique approach to large dimer). The Al_3 system (in which three-body interactions occur) was investigated separately to evaluate the importance of different many-body terms. For the cases presented in Table X the S and BA methods give very similar ΔE_i^k (the BA method gives the smallest errors for Al_3). It is interesting to notice that for Al_{13} all TB methods considered in this paper correctly predict the lowest energy to be the icosahedron (structure No. 1).

Mean unsigned errors for the ionization potentials calculated by TB methods are given in Table XI. One can see that the ionization potentials are reproduced with an error less than 10% for all methods. This means that neither the number of optimized parameters nor the choice of many-body terms has much influence on the values of the calculated IPs, which are realistic (though not quantitatively accurate) for all Slater-Koster-type and MBTB methods.

As in two previous papers[11,16] we calculate the cohesive energy for several quasispherical clusters. The results are

shown in Table XII. The rate of approach to the bulk value of 3.43 eV is remarkably similar across the various models.

It is interesting to compare the present TB results to the TBTE model of Mehl and Papaconstantopoulos. As discussed in Ref. 11, their method is very inaccurate if any Al-Al distance is smaller than 2.25 Å. (However, their method was not designed to be valid in that region, and it is very reasonable that a model is parametrized for a specific objective and is not equally valid for all properties and all geometries.) The mean unsigned errors for both data sets are compared in Table XIII. The present models clearly represent a qualitative advance, even for nonclose geometries, where our best model reduces the mean error by more than an order of magnitude.

Our models do not have a cutoff. Therefore, it is interesting to consider the ranges of the two-body functions that result from the parametrizations presented in this paper. In the WH, EWH, and OWH models, the two-body functions are $V_{l_i l_j \lambda}$ and V_{rep}, whereas in the CN, BA, and S models, the two-body functions, say $f(R)$, are given by $V_{l_i l_j} F^{\text{MB}}$ and $V_{\text{rep}} F^{\text{MB}}$. The ranges of these functions may be illustrated by tabulating $f(R_{\alpha\beta}^{(n)})/f(R_{\alpha\beta}^{(1)})$ where $f(R_{\alpha\beta}^{(n)})$ is the nth nearest neighbor distance in the bulk FCC lattice. (Thus $R_{\alpha\beta}^{(1)}$ is $a_{\text{exp}}/\sqrt{2} = 2.863$ Å, and $R_{\alpha\beta}^{(2)}$, $R_{\alpha\beta}^{(3)}, \dots$ are $4.050, 4.960, \dots$ Å.) These ratios were determined for the cental atom of a 603-atom quasispherical lattice and are tabulated in Table XIV. The table shows that the two-body repulsion functions decrease more rapidly than the Hamiltonian matrix elements, and in all cases they are less than 1% of their nearest-neighbor values by the third-nearest-neighbor distance $R_{\alpha\beta}^{(3)}$. The average value of the Hamiltonian matrix elements at $R_{\alpha\beta}^{(3)}$ is however 11% as large as at $R_{\alpha\beta}^{(1)}$. Although some older models neglect the Hamiltonian matrix elements beyond the second nearest neighbors, our model has much longer-ranged interactions.

Finally we consider a comparison of the present results to the analytic potential results of Ref. 16. This is done in Table XV. We see that the pairwise approximation is much better in the context of TB theory than for analytic potentials. Incorporating the pairwise approximation into the matrix elements, followed by diagonalization of the TB Hamiltonian automatically builds in most of the many-body effects. However, we can still reduce the error by another 50% by explicit inclusion of many-body effects in the matrix elements, as we anticipated in Sec. II.

Cost comparisons (computer times) are given in Table XVI. For pure Al, the analytic potentials are much less expensive. However, once one considers systems containing other elements such as H and C, along with Al, it may be harder to "discover" functional forms that incorporate the many-body effects. One can anticipate that TB will still include a good portion of the many-body effects automatically, but it is a question for future study.

VI. CONCLUDING REMARKS

In a previous study,[16] we (and Jasper) tested a large number of analytic potential energy functions, for example, pairwise additive,[48,49] nonpairwise additive,[50,51] and embedded-atom (EA)-type[52–55] methods, for Al clusters. In both that work and the present study we based our conclusions primarily on the average unsigned error per atom in the atomization energy, averaged over Al_2, Al_3, Al_4, Al_7, Al_{13}, and bulk Al. Thus the studies can be directly compared. The best previous potential energy functions were found to have mean error of 0.45 eV/atom for pairwise additive, 0.16 eV/atom for nonpairwise additive, and 0.13 eV/atom for EA-type, and reoptimization of these kinds of potential energy functions against our new cluster data training set reduced the error for these three categories of potentials to 0.31, 0.13, and 0.046 eV/atom, respectively.[16] In the present work we found that the best tight-binding model with pairwise matrix elements (we call this Slater-Koster-type TB) has a mean error of only 0.056 eV/atom. Thus the tight-binding formalism by lodging the pairwise functions in a quantum mechanical framework immediately recovers almost all of the many-body effects that can be recovered even by the very best and most sophisticated analytic potential energy functions. Then by explicitly adding many-body effects to the Hamiltonian, we can do even better. In particular, we found that the screening function introduced by Ho and co-workers is very powerful, and our final model which includes this function has a mean error of only 0.029 eV.

It is especially noteworthy that we achieved this accuracy without including the overlap matrix in the secular equation. Thus our model is what some workers refer to as "orthogonal tight-binding," and this is well known to more efficient for molecular dynamics calculations than nonorthogonal tight-binding.

We expect that the present model will be particularly useful for simulating nonbulk Al, for example, Al nanoparticles, since we placed an emphasis on interpolating between clusters and the bulk rather than on quantitatively reproducing a full set of bulk properties. However, the approach is general and we recommend the many-body tight-binding with screening (MBTB-S) scheme for other applications to Al and other elements. It can also serve as a starting point for parametrizing heteronuclear systems such as the interaction of hydrocarbon fragments with Al particles.

*Visiting researcher, Department of Chemistry, University of Minnesota, 2002–2003.

[1] J. C. Slater and G. F. Koster, Phys. Rev. **94**, 1498 (1954).

[2] D. W. Bullett, Solid State Phys. **35**, 129 (1980).

[3] C. Z. Wang and K. M. Ho, Adv. Chem. Phys. **93**, 651 (1996).

[4] L. Colombo, Annu. Rev. Comput. Phys. **4**, 147 (1996).

[5] C. M. Goringe, D. R. Bowler, and E. Hernández, Rep. Prog. Phys. **60**, 1447 (1997).

[6] *Tight-Binding Approach to Computational Materials Science*, edited by P. E. A. Turchi, A. Gonis, and L. Colombo (Materials Research Society, Warrendale, PA, 1998).

[7] K. Masuda-Jindo, Mater. Trans., JIM **42**, 979 (2001).

[8] D. A. Papaconstantopoulos and M. J. Mehl, J. Phys.: Condens. Matter **15**, R413 (2003).

[9] A. P. Horsfield and A. M. Bratkovsky, J. Phys.: Condens. Matter **12**, R1 (2003).

[10] T. Liu, Ph.D. thesis, University of Minnesota, Minneapolis, 2000; T. Liu and D. G. Truhlar (unpublished).

[11] N. E. Schultz, G. Staszewska, P. Staszewski, and D. G. Truhlar, J. Phys. Chem. B **108**, 4850 (2004).

[12] M. S. Tang, C. Z. Wang, C. T. Chan, and K. M. Ho, Phys. Rev. B **53**, 979 (1996).

[13] H. Hass, C. Z. Wang, M. Fähnle, C. Elsässer, and K. M. Ho, Phys. Rev. B **57**, 1461 (1998).

[14] D. Nguyen-Mahn, D. G. Pettifor, and V. Vitek, Phys. Rev. Lett. **85**, 4136 (2000).

[15] S. R. Nishitani, S. Ohgushi, Y. Inoue, and H. Adachi, Mater. Sci. Eng., A **309–310**, 490 (2001).

[16] A. W. Jasper, P. Staszewski, G. Staszewska, N. E. Schultz, and D. G. Truhlar, J. Phys. Chem. B **108**, 8996 (2004).

[17] R. W. Numrich and D. G. Truhlar, J. Phys. Chem. **79**, 2745 (1975).

[18] I. Cerdá and F. Sesia, Phys. Rev. B **61**, 7965 (2000).

[19] Y. Wang and C. H. Mak, Chem. Phys. Lett. **235**, 37 (1995).

[20] E. Lomba, D. Molina, and M. Alvarez, Phys. Rev. B **61**, 9314 (2000).

[21] J. Hubbard, Proc. R. Soc. London, Ser. A **276**, 238 (1963).

[22] *Handbook of Chemistry and Physics*, 78th ed., edited by D. R. Lide (CRC Press, Boca Raton, FL, 1997); C. E. Moore, *Atomic Energy Levels as Derived from the Analyses of Optical Spectra*, Circular of the National Bureau of Standards 467 (US Department of Commerce, Washington, DC, 1949), Vol. 1.

[23] R. S. Mulliken, J. Chim. Phys. Phys.-Chim. Biol. **46**, 497 (1949).

[24] M. Wolfsberg and L. Helmholtz, J. Chem. Phys. **20**, 837 (1952).

[25] R. Hoffmann, J. Chem. Phys. **39**, 1397 (1963); **40**, 2047 (1964); **40**, 2474 (1964); **40**, 2480 (1964); **40**, 2745 (1964).

[26] E. Clementi and D. L. Raimondi, J. Chem. Phys. **38**, 2686 (1963).

[27] H. W. Jones, Int. J. Quantum Chem. **19**, 567 (1981).

[28] W. A. Harrison, *Elementary Electronic Structure* (World Scientific, Singapore, 1999).

[29] E. Hückel, Z. Phys. **70**, 204 (1931); J. P. Lowe, *Quantum Chemistry* (Academic, New York, 1993).

[30] M.-H. Whangbo, M. Evain, T. Hughbanks, M. Kertesz, S. Wijeyesekera, C. Wilker, C. Zheng, and R. Hoffmann, Quantum Chemistry Program Exchange, Indiana University, 1987, No. 571.

[31] T. Liu and D. G. Truhlar, EHT-version 1.0: A Program for Extended Hückel Theory, University of Minnesota, Minneapolis, MN, 2000. See http://t1.chem.umn.edu/eht

[32] S. Serra, C. Molteni, and L. Miglio, J. Phys.: Condens. Matter **7**, 4019 (1995).

[33] C. Z. Wang, B. C. Pan, and K. M. Ho, J. Phys.: Condens. Matter **11**, 2043 (1999).

[34] H. Nakamura, D. Nguyen-Manh, and D. G. Pettifor, J. Alloys Compd. **306**, 113 (2000).

[35] N. A. Marks, Phys. Rev. B **63**, 035401 (2001).

[36] N. Marks, J. Phys.: Condens. Matter **14**, 2901 (2002).

[37] R. Gaudoin, W. M.C. Foulkes, and G. Rajagopal, J. Phys.: Condens. Matter **14**, 8787 (2002).

[38] *American Institute of Physics Handbook*, 3rd ed., edited by M. W. Zemansky and D. E. Gray (McGraw-Hill, New York, 1972).

[39] W. C. Stwalley and M. de Llano, Z. Phys. D: At., Mol. Clusters **2**, 153 (1986).

[40] W. H. Qi, M. P. Wang, and G. Y. Xu, Chem. Phys. Lett. **372**, 632 (2003).

[41] J. P. Perdew, M. Ernzerhof, and K. Burke, J. Chem. Phys. **105**, 9982 (1996).

[42] N. E. Schultz and D. G. Truhlar, J. Chem. Theory Comput. (to be published).

[43] See EPAPS Document No. E-PRBMDO-70-106448 for suplementary information including the energies and multiplicities of aluminum clusters calculated by all eight tight-binding methods considered in this paper and two sets of adjustable parameters for MBTB-S method optimized for penalty energies of 0.0 eV and 0.64 eV. A direct link to this document may be found in the online article's HTML reference section. The document may also be reached via the EPAPS homepage (http://www.aip.org/pubservs/epaps.html) or from ftp.aip.org in the directory /epaps/. See the EPAPS homepage for more information.

[44] J. P. Perdew and A. Zunger, Phys. Rev. B **23**, 5048 (1981).

[45] C. A. Coulson and I. Fischer, Philos. Mag. **40**, 386 (1949).

[46] D. L. Carroll, in *Developments in Theoretical and Applied Mechanics*, edited by H. Wilson, R. Batara, C. Bert, A. Davis, R. Schapery, D. Stewart, and F. Swinson (School of Engineering, University of Alabama, Tuscaloosa, Alabama, 1996), Vol. XVII, p. 411.

[47] D. L. Carroll, GA-version 1.7a: FORTRAN Genetic Algorithm Driver, CU Aerospace, Urbana, IL, 2001. See http://cuaerospace.com/carroll/ga.html

[48] D. G. Pettifor and M. A. Ward, Solid State Commun. **49**, 291 (1984).

[49] P. de Sainte Claire, G. H. Peslherbe, and W. L. Hase, J. Phys. Chem. **99**, 8147 (1995).

[50] Ş. Erkoç, Phys. Status Solidi B **155**, 461 (1989).

[51] H. Cox, R. L. Johnston, and J. N. Murrell, Surf. Sci. **373**, 67 (1997).

[52] H. Gollisch, Surf. Sci. **166**, 87 (1986).

[53] J. Mei, J. W. Davenport, and G. W. Fernando, Phys. Rev. B **43**, 4653 (1991).

[54] F. H. Streitz and J. W. Mintmire, Phys. Rev. B **50**, 11996 (1994).

[55] Y. Mishin, D. Farkas, M. J. Mehl, and D. A. Papaconstantopoulos, Mater. Res. Soc. Symp. Proc. **538**, 535 (1999).